Thermodynamic Evaluation of Binding Interactions in the Methionine Repressor System of *Escherichia coli* Using Isothermal Titration Calorimetry†

David E. Hyre‡ and Leonard D. Spicer*,‡,§

Departments of Biochemistry and Radiology, Duke University Medical Center, Durham, North Carolina 27710

Received August 26, 1994; Revised Manuscript Received December 6, 1994⊗

ABSTRACT: The binding interactions of the methionine repressor protein, MetJ, from *Escherichia coli* with its cognate, metbox DNA sequence and corepressor *S*-adenosylmethionine were examined using calorimetric methods. A detailed thermodynamic characterization of this system which exhibits the recently reported $(\beta\alpha\alpha)_2$ binding motif provides values for ΔG, ΔH, and ΔS for each step in the repressor binding cycle. These studies show that, in the presence of corepressor, MetJ binds to a single metbox operator site with $\Delta G = -7.7$ kcal·mol^{-1}, whereas in the absence of corepressor, the free energy of interaction with a single site is -5.8 kcal·mol^{-1}. Cooperative interactions between two repressor molecules bound to two adjacent sites contribute an additional free energy of -1.3 kcal·mol^{-1} to binding at the second site. Binding is enthalpically unfavorable in the absence of the corepressor with $\Delta H = +2.6$ kcal·mol^{-1} but becomes exothermic with $\Delta H = -4.6$ kcal·mol^{-1} when corepressor is present. The heat capacity for the system decreases significantly by $\Delta C_p = -290$ cal·mol^{-1}·K^{-1} on a per site basis when the protein binds to DNA, and interactions between repressor molecules bound to adjacent sites contribute a $\Delta C_p = -800$ cal·mol^{-1}·K^{-1}, indicating that solvent exclusion plays a significant role in binding in this system. The corepressor binds to the unbound repressor protein with a free energy of $\Delta G = -6.0$ kcal·mol^{-1} and to the MetJ−operator complex with $\Delta G = -6.95$ kcal·mol^{-1}. Repressor binding to random-sequence DNA was estimated to occur with a free energy of -5.7 kcal·mol^{-1} in the presence of corepressor. These data clearly indicate that MetJ repressor dimer binds specifically to the central region of its 8 bp cognate metbox operator but recognizes partial operator sequences as short as 6 bp. Cooperativity in binding of adjacent MetJ dimers to a double metbox sequence is demonstrated to be important in determining the energetics of the interaction. Finally, the corepressor *S*-adenosylmethionine enhances the affinity of MetJ for its recognition site DNA by a factor of 25 and contributes significantly to the net exothermicity of repressor binding.

The methionine repressor protein from *Escherichia coli* (MetJ)[1] controls transcriptional levels of enzymes in the methionine biosynthetic pathway by binding to DNA operator sequences preceding the structural genes. Binding of MetJ to recognition sequences in DNA is enhanced by a corepressor, *S*-adenosylmethionine (SAM). This overall mechanism for repression of the biosynthetic path for methionine is illustrated schematically in Figure 1 (Cohen & Jacob, 1959; Saint-Girons et al., 1994, 1986, 1988; Old et al., 1991). There are a number of naturally occurring operator sequences from which a palindromic consensus MetJ binding site has been culled (Belfazia et al., 1986; Saint-Girons et al., 1986). This sequence, 5′-AGACGTCT-3′, is often referred to as a "metbox". Wild-type operator sequences have two to five contiguous 8 bp sites, which show varying homology to the consensus sequence, suggesting that multiple binding may be necessary for biological function.

A number of studies have been reported on the interactions of MetJ with both wild-type and consensus operator sequences, in which the proposed MetJ binding site is centered on the junction between metboxes (Saint-Girons et al., 1986; Davidson & Saint-Girons, 1989; Phillips et al., 1989). The X-ray structure of the protein−DNA cocrystal, however, shows binding in the center of each metbox (Somers & Phillips, 1992).

Methionine operator sequences linked to a β-galactosidase reporter gene show that two contiguous metboxes are sufficient for repression of *in vivo* transcription by MetJ, while filter-binding studies show that a single metbox sequence has a marked reduction in repressor binding (Phillips et al., 1989). DNase protection and chemical modification studies also suggest that MetJ contacts a 12−16 bp region of DNA symmetric about the center of a two-metbox operator sequence (Davidson & Saint-Girons, 1989; Phillips et al., 1989). These studies suggest in addition that the range of control exerted on the system is proportional to the number of metboxes present in the operator region (Saint-Girons et al., 1984, 1986; Davidson & Saint-Girons, 1989).

The MetJ protein forms a homodimer of 12 kDa monomer units (Saint-Girons et al., 1986; Rafferty et al., 1989). Medium- to high-resolution crystal structures are available for the protein: without corepressor, apoMetJ; with SAM, holoMetJ (Rafferty et al., 1989); and bound to its DNA recognition sequence with SAM (Somers & Phillips, 1992).

† This work was supported in part by the National Institutes of Health under Grant RO1GM41829.

* Address correspondence to this author.
‡ Department of Biochemistry.
§ Department of Radiology.

⊗ Abstract published in *Advance ACS Abstracts,* February 1, 1995.

[1] Abbreviations: ITC, isothermal titration calorimetry; SAM, *S*-adenosylmethionine; MetJ, methionine biosynthetic repressor protein dimer; apoMetJ, repressor dimer with nothing bound; holoMetJ, repressor dimer with two bound SAM; bp, base pairs of double-stranded DNA; metbox, 8 bp DNA operator sequence for MetJ; MIS, multiple independent site.

0006-2960/95/0434-3212$09.00/0

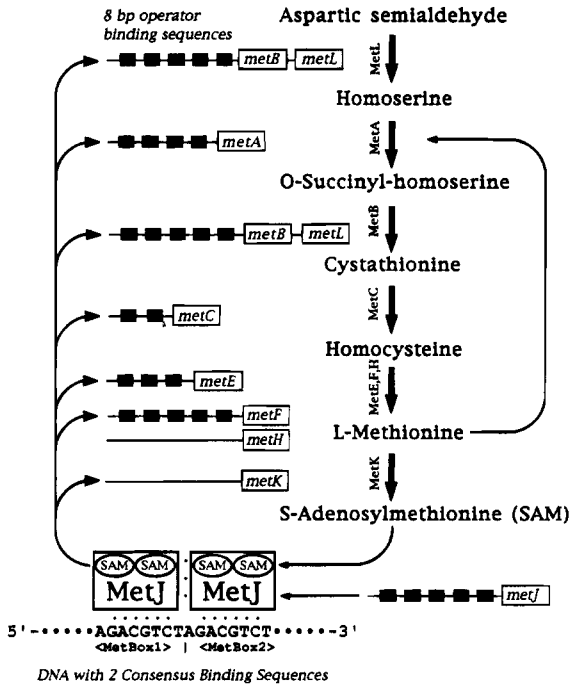

FIGURE 1: Biosynthetic and regulatory pathway for methionine biosynthesis. Enzymes, encoded by the structural genes indicated in open boxes, convert aspartic semialdehyde to methionine, which can be further modified through adenylation to *S*-adenosylmethionine (SAM). Most of the genes for the eight enzymes that accomplish this synthesis contain operator sites made up of multiple 8 bp segments, represented by the dark boxes, each having varying homology to the "metbox" consensus sequence 5′-AGACGTCT-3′ (Belfazia et al., 1986; Saint-Girons et al., 1988; Phillips et al., 1989; Old et al., 1991). The operators place the genes under the control of the MetJ repressor protein and the pathway end product SAM.

These structures reveal that the protein binds as a dimer to the DNA, inserting two β-strands into the major groove, with the center of each binding site aligned with the center of each metbox sequence. MetJ dimers bound to neighboring metboxes interact with one another through α-helical contacts involving the first of three helices in each monomer. Each MetJ dimer symmetrically binds two molecules of SAM on the side of the protein opposite the DNA binding site, in both the presence and absence of bound DNA. In the three different crystal structures of the three forms of the protein dimer, there are no significant differences in the secondary and tertiary structures of the protein which might provide a structural rationale for the allosteric enhancement of DNA binding observed upon addition of SAM.

The components of the MetJ system represent three types of binding interactions: protein−SAM (corepressor), protein−DNA (operator sites), and protein−protein (neighboring dimers). These interactions modulate transcription of the biosynthetic enzymes and thus repress methionine production as a result of fluctuations in the levels of the end product SAM. An understanding of the energetics in this system provides insight into this and other biological control mechanisms and may facilitate the calibration of structure-based thermodynamic models. To date, however, a detailed investigation of the binding energetics in the MetJ system has not been undertaken. Earlier studies focused on measuring binding affinities for substrates with multiple metboxes and have suffered from secondary binding events to nonoperator DNA and the formation of higher order complexes that bind more than one MetJ dimer per metbox (Saint-Girons et al., 1986, 1988; Phillips et al., 1989; Kirby and Greene, personal communication). Recently, a communication has been published describing calorimetric results for selected pathways of the MetJ system (Cooper et al., 1994). These data are interpreted with a simplified, noncooperative model, however, which does not adequately account for known protein−protein interactions in the system.

The calorimetric studies reported here give thermodynamic data for the molecular interactions associated with the overall repression mechanism of MetJ and its modulation by corepressor SAM including binding site recognition, affinity, and cooperativity. Of particular interest is the first extensive thermodynamic characterization of the binding cycle for the recently reported β-strand DNA binding motif exhibited by the MetJ repressor protein (Phillips, 1991; Phillips et al., 1993). These thermodynamic quantities are interpreted in terms of a model for the MetJ system, incorporating hydration, nonspecific affinity for DNA, cofactor binding, and cooperativity between neighboring sites.

EXPERIMENTAL PROCEDURES AND THERMODYNAMIC MODELS

Methionine repressor protein was expressed from the pET-MetJ plasmid, kindly provided by R. C. Greene and T. Kirby, in the BL21-DE3 overexpression system (Studier & Moffatt, 1986; Kirby and Greene, personal communication), with the pLysE plasmid present. The protein was purified using the method of Kirby and Greene (personal communication), in which the clarified cell lysate is treated with 45% and 95% saturated ammonium sulfate, the 95% pellet is resuspended and desalted on a 200-cm^3 Sephacryl S-200 column, and the protein is bound to and eluted from a 80-cm^3 hydroxyapatite column using a 0.05−0.6 M K_2HPO_4, pH 7, linear gradient. This method was modified for our purposes in the following way. The Sephacryl S-200 column was replaced by a G-50 column to retard smaller contaminants, and the protein was lyophilized in proportionally diluted buffer in order to maintain sufficient salt and buffer concentrations during the concentration that occurs upon lyophilization. In the absence of salt, lyophilization destabilized the protein, leading to a significant amount of denatured material upon resuspension of the sample. The protein concentration was determined by absorption at 280 nm using an extinction coefficient of 15 380, corresponding to 0.78 mg·mL^{-1} A_{280}^{-1} cm^{-1} (Smith et al., 1985), the value of which was confirmed by a denaturing assay (Edelhoch, 1967). All protein solutions were prepared for calorimetric or spectroscopic study by dissolving lyophilized stock material in water and dialyzing into the standard buffer solution. This was followed by centrifugation and filtration to remove particulates. Protein solutions ranged between 0.6 and 1.5 mM (dimer).

DNA substrates were obtained from Oligos Etc. Three of the oligonucleotides were designed to contain an integral number of metboxes plus two additional base pairs of "anti"-metbox at each end to prevent additional binding or distortion of the binding sites. The anti-metbox sequence is designed to prevent additional nonspecific binding of MetJ to sequences outside of the metboxes (Phillips et al., 1989). Three sequences were used: (1) single-metbox DNA 5′-GGAGACGTCTCC-3′, (2) double-metbox DNA 5′-GGAGACGTCTAGACGTCTCC-3′, and (3) frame-shifted double-

metbox DNA having one metbox centered between two half-metboxes 5′-GGGTCTAGACGTCTAGACCC-3′. Random-sequence 12 bp oligonucleotides were also generated, with full degeneracy at all bases. Oligonucleotides were chemically synthesized and determined to be pure by gel electrophoresis and NMR spectroscopy. The inherent palindromic nature of the metbox created the potential for hairpin formation, as the oligonucleotides were entirely self-complementary, but only a single species was seen in one-dimensional NMR spectra at 100 μM duplex concentration, with resonance line widths consistent with a molecular weight corresponding to the double-stranded species. In addition, the observed resonances were consistent with the expected number of base pairs with no unpaired bases, displaying chemical shift patterns matching those of previously assigned duplex metbox constructs. DNA concentrations were determined by optical absorption at 260 nm using sequence-corrected extinction coefficients of 164 400 and 269 600 for the single- and double-site molecules, corresponding to 21.7 and 22.2 mg·mL^{-1} A_{260}^{-1} cm^{-1} (Cantor & Schimmel, 1980). All DNA samples were prepared by dissolving the dried material at high concentration in buffer, followed by centrifugation and filtration. Sample concentrations ranged from 30 to 250 μM duplex molecules. The double-metbox $(MetJ)_2$−DNA complex was prepared by adding 400 μL of 1 mM MetJ to 1.6 mL of 500 μM double-metbox DNA, equilibrating overnight, removing any precipitate by centrifugation, and quantitating the concentrations of both components by optical absorbance measurements and multiple-wavelength deconvolution.

Samples were further prepared for calorimetric measurement by dialyzing the macromolecules into a standard salt solution containing 50 mM KCl, 40 mM NaCl, 10 mM NaI, 5 mM MgCl, 2 mM DTT, and 2 mM NaN_3, with the pH adjusted to 7 with HCl and NaOH. The strong optical absorbance of SAM prevented accurate determination of macromolecule concentrations in samples containing SAM; therefore, the samples were first dialyzed into the common solution and were then augmented by addition of SAM after measurement of the macromolecule concentrations. Either 25 mM Tricine or 20 mM Na_2HPO_4 plus 5 mM KH_2PO_4 buffers, with their pH adjusted to 7.0 using HCl and NaOH, were added after dialysis. Using this alternate method, the baseline solvent dilution heats measured during titration did not increase appreciably, and final concentrations could be determined accurately. All samples were degassed under vacuum immediately before use.

Thermodynamic measurements were carried out on the MetJ repressor system using isothermal titration calorimetry (ITC). Experimental parameters that were explored included DNA sequence and length, cofactor SAM concentrations, temperature, and pH buffer system. SAM was used in corepressor binding studies at a concentration of 2 mM, 10-fold higher than the reported K_d of 200 μM (Saint-Girons et al., 1986, 1988). This concentration was determined to be optimal for binding based on a series of ITC experiments carried out at SAM concentrations from 0 to 10 mM. SAM concentrations above 2 mM were not used because elevated levels of SAM showed nonlinear heat evolution, which was ascribed to nonspecific interactions with the DNA. Calorimetry was performed in a MicroCal Omega 2 isothermal titration calorimeter fitted with a Kiethly nanovoltometer as a null detector. DNA served as the substrate and MetJ as the injected ligand in all experiments except the binding of SAM to the MetJ−double-metbox complex, in which the complex served as the substrate and SAM as the ligand. Injections were performed as quickly as possible, each lasting 2−20 s, in increments of 2−40 μL apiece, while stirring at 400 rpm, with a 5-min equilibration period between each injection. The ITCArea program (Johns Hopkins BioCalorimetry Center) was used for numerical integration of the heat flow data and allowed for linear compensation of baseline drifts by extrapolation of the pre- and postpeak baseline. The resulting series of heats was then used directly without further modification in the fitting procedure. Calorimetric data were fit within Microsoft Excel using an iterative differential, nonlinear least squares error minimization procedure developed in our laboratory, with the model appropriate to the number of binding sites present per substrate as described below. Asymmetric confidence intervals for the fitted parameters were determined by the support plane method (Johnson, 1983; Johnson & Frasier, 1985), using the F test for 90% confidence ($p = 0.1$) to determine the interval limits. The reported intervals represent the larger of the two asymmetric intervals.

Qualitative modeling of hydration changes employed the solvation function of the Biosym Insight software package and was based solely on the operator−holoMetJ crystal structure referenced in the Brookhaven Protein Data Bank as pdb1cma (Somers & Phillips, 1992). The structure was divided into three parts (two dimers and one double-metbox DNA), all possible permutations were solvated with a 3 Å shell of hydration, and the number of "bound" water molecules was counted and compared. Data are not shown due to the strictly qualitative nature of this simulation.

BINDING MODELS

The binding models used to fit the calorimetric data are described below. Additional information on these models is available as supplementary material. The term X in these models refers to the concentration of MetJ protein dimers, the ligand, and the term M refers to duplex DNA concentration, the substrate, since in practice aliquots of MetJ were injected into a solution of DNA for most of the binding experiments.

The experimentally measured calorimetric heat is presented in terms of the binding polynomial for the model under consideration. The binding polynomial describes bound species by the sum of the relative populations of each bound state M_i, with its characteristic relative free energy ΔG_i and related association constant K_{ai} (Wyman & Gill, 1990; Bains & Freire, 1991; Cantor & Schimmel, 1980). The least complex multiple independent site (MIS) model incorporates a quantity, n, of one type of ligand binding site having an intrinsic associative equilibrium constant K_a

$$P_{MIS} = (1 + K_a X_f)^n \quad (1)$$

The total observed calorimetric heat is then the sum of the heats for the formation of each bound species

$$\langle \Delta H \rangle = \frac{(nK_a X_f \Delta H)}{(1 + K_a X_f)} \quad (2)$$

Under the experimental conditions of limiting amounts of

ligand, the free ligand concentration X_f and free substrate concentration M_f are obtained analytically from the mass balance equations relating the total quantity of each molecule to the sum of the free and bound quantities.

Thus the measured heat of the reaction following each injection can be described by a function that depends only on X_t, M_t, n, K_a, and ΔH, of which the quantities X_t and M_t are known. The calorimetric data are iteratively fit for n, ΔH, and K_a on the basis of the known values of X_t and M_t at each point in the titration. ΔG for the reaction is then related to K_a, ΔH, and ΔS by the standard equation

$$\Delta G = -RT \ln K_a = \Delta H - T\Delta S \quad (3)$$

The constant-pressure heat capacity change upon binding, ΔC_p, is determined by the temperature dependence of ΔH and is equal to the slope in a linear fit of ΔH versus temperature

$$\Delta C_p = \frac{\partial H}{\partial T} \quad (4)$$

The cooperative binding energy from adjacent bound ligands was estimated on the basis of an extension of the two-site MIS model incorporating an additional contribution to ΔG and ΔH from cooperativity, Δg_c and Δh_c. In this model eq 5 includes an additional term κ for the DNA molecules with two bound MetJ, which modifies the relative population of the doubly bound state to give

$$P_{\text{Coop-2}} = 1 + 2K_aX_f + K_a^2\kappa X_f^2 \quad (5)$$

where κ is related to Δg_c as K_a is to ΔG:

$$\Delta g_c = -RT \ln \kappa \quad (6)$$

The excess molar enthalpy $\langle \Delta H \rangle$ for the reaction includes terms containing the single-site intrinsic ΔH for each bound ligand and an additional cooperative Δh_c for the doubly bound species as indicated:

$$\langle \Delta H \rangle = \frac{2K_aX_f\Delta H + K_a^2\kappa X_f^2(2\Delta H + \Delta h_c)}{1 + 2K_aX_f + K_a^2\kappa X_f^2} \quad (7)$$

It is noted that, in this model, if $\Delta g_c = 0$ ($\kappa = 1$) and $\Delta h_c = 0$, the equations become identical to the MIS model with $n = 2$.

In the fitting of calorimetric data to these binding models, the presence of two different asymptotes improves the reliability of binding affinity (K_a) and enthalpy parameters determined by the curve-fitting procedure, since the curvature of the transition is determined by the association constant, and the starting asymptote is determined by the enthalpy. Association constants cannot be reliably determined for thermograms without curvature, as occurs under conditions of total association at partial saturation, and enthalpies are not well-defined for curves without an observable starting asymptote but can be determined if *a priori* information is available about binding stoichiometry (Wiseman et al., 1989).

RESULTS

Single-Metbox Binding. Isothermal titration calorimetry (ITC) follows the binding of ligand to substrate by measuring the evolution or uptake of heat due to a change in binding

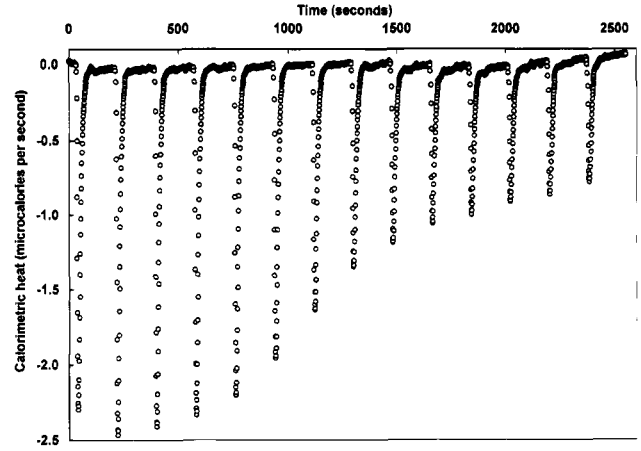

FIGURE 2: Typical raw thermogram for the binding of MetJ to a single-metbox oligonucleotide at 35 °C in the presence of SAM. MetJ was injected stepwise into DNA, with each injection performed as quickly as possible and followed by a 5-min reequilibration period. The electrical current required to compensate for changes in heat flow was digitally sampled every second. Although the peak heights approximate a sigmoidal binding curve, accurate quantitative characterization requires the determination of the area underneath each peak which in these studies was accomplished by numerical integration.

saturation, which is caused by the injection of additional ligand into the substrate solution. A typical thermogram for binding of MetJ to a single-site duplex DNA fragment at 35 °C with 2 mM SAM is shown in Figure 2. The negative sign of the measured heat indicates that the enthalpy change for each injection is negative and the binding is exothermic. The binding curve determined by the peak areas in Figure 2 is sigmoidal, indicating that not all injected molecules bind to substrate. After multiple injections the binding curve asymptotically approaches a constant baseline, defined by the heat of dilution, which shows that the titration was taken to near completion. The processed thermogram data for the above example and the other 12 bp oligonucleotides studied are shown in Figure 3 along with curves that represent the best fit to the multiple independent site model described above.

The single-site DNA ITC titration data obtained in these studies were fit to the multiple independent site (MIS) model described above, on the basis of the assumption that any binding sites present on the DNA are independent and noninteracting. An iterative nonlinear least squares curve-fitting program was used to fit the data to the binding curve described by eqs 1 and 2 in the following way. The total heat content after each injection was described by the product of the number of binding sites, substrate concentration, estimated enthalpy change, cell volume, and estimated fractional saturation of sites from eqs 1 and 2. The observed calorimetric heats were described by the change in total heat content in eq 2 caused by injection of additional ligand.

The quality of the fitting procedure is illustrated by the curves in Figure 3. Thermodynamic parameters derived from this analysis are tabulated in Table 1. It should be pointed out that the fitting strategy employed takes into account the progressive dilution of X_t and M_t due to the additional injected volume and that only functional binding unit concentrations are used; i.e., MetJ concentrations were calculated as dimer quantities, and oligonucleotides were calculated as duplex molecules. Controls were established by injecting MetJ into plain buffer without DNA present and

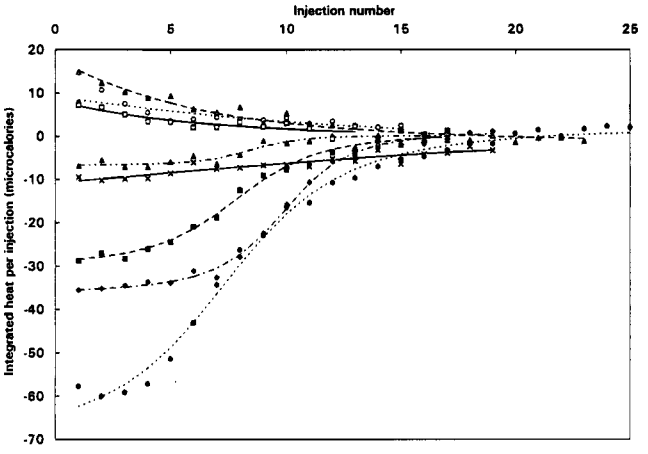

FIGURE 3: Integrated calorimetric heats (individual points) and best-fit curves to a multiple independent site model for all 12 base-pair molecules listed in Table 1 (see table for symbols). All data acquired in the presence of SAM (filled symbols plus ×'s) are negative, indicating an exothermic reaction, while those without SAM (open symbols) are all positive and endothermic. Note that all metbox DNA with SAM are sigmoidal due to their larger K_a, while the others lack an inflection due to a smaller K_a. It is not uncommon for the heat measured during the first injection to be inaccurate due to imprecision of alignment between the stepper motor and the syringe plunger for the first injection.

in all cases showed a constant heat of dilution. The heat of dilution varies between experiments due to imprecision in matching the buffer conditions between the calorimeter cell and the injection syringe, since samples are prepared by dilution and mixing of stock solutions (see Experimental Procedures). An internal calibration procedure was used to correct for this imprecision, resulting in a constant baseline that was added as a constant heat for each injection. As modeled in the above equations, the data were directly fit in their derivative form ($\Delta Q_i/\Delta X_t$) and not as the integrated total heat, thereby avoiding the accumulated errors caused by summation of the measured heats. Figure 3 shows that all data obtained in the presence of SAM are well fit by the MIS model and give n values close to 1 as reported in Table 1. The fit to data obtained in the absence of SAM was sensitive to the starting values of the adjustable parameters n, K_a, ΔH, and the heat of dilution but converge if n was held equal to one binding site, consistent with the titrations in the presence of SAM, the model under consideration, and nuclease protection assays, in which MetJ specifically binds to and protects metbox sequences from digestion even in the absence of SAM (Kirby and Greene, personal communication).

Titrations carried out in the presence of SAM indicated an exothermic binding process. The fitted values of ΔH for the single-metbox titrations decreased in an approximately linear fashion with decreasing temperature, yielding a value for the heat capacity change of $\Delta C_p \approx -0.3$ kcal·mol^{-1}K^{-1}. In contrast, the reactions carried out in the absence of SAM were all endothermic and were characterized by a lower binding affinity (K_a), as evidenced by a less negative ΔG. Agreement of the results in the three equivalent experiments reported in Table 1 reinforces this observation. One of the three experiments in the absence of SAM utilized the pH buffer molecule Tricine in place of phosphate to examine changes in protonation upon binding. Tricine has a larger enthalpy of ionization than does phosphate (+7.66 versus +1.00 kcal·mol^{-1}·K^{-1}; Murphy et al., 1993), so that release or uptake of protons during the course of the reaction would result in a significantly different measured enthalpy. This is not observed in the presence of Tricine as shown in Table 1. ΔC_p was not measured in the absence of SAM due to instability of the apoMetJ−DNA complex.

Alternate Sequence Binding. Nonspecific binding of MetJ to nonoperator DNA was estimated by titration of protein into a solution of 12 bp random-sequence oligonucleotides in the presence of SAM. The reaction was exothermic, as in the experiments with operator DNA and SAM, but ΔG was significantly less negative for the randomized sequence. The observed curve clearly does not show the same sigmoidal behavior as that observed for the single-metbox titration with SAM at 10 °C. Fitting of these data was also sensitive to the starting values of the adjustable parameters and did not converge unless the heat of dilution was set equal to the value of the last data point. This approach is based on the assumption that the reaction was near completion and that the only heat measured from the last injection was the heat of dilution. With these assumptions the best fit to n was approximately 1.6 ± 0.3. The binding observed is considered to be nonspecific due to the poorly determined value of n, as expected for a mixture of oligonucleotides with randomized sequences.

An additional control experiment was conducted with a 20 bp oligonucleotide with a sequence frame-shifted by half a metbox, consisting of the 3′ half of one metbox, one full metbox, and the 5′ half of a metbox in that order. This titration (data not shown) was used to check the sensitivity of the fitting equations to changes in n and to confirm that the length of the DNA was not determining the number of binding sites. The data yield a ΔG of −8.7 ± 0.4 kcal·mol^{-1} when fit to the MIS model, similar to that of the single-metbox constructs, with $n = 2.69 \pm 0.06$, showing that three MetJ dimers are binding to the DNA, most likely one to the central metbox and two to the half-metboxes plus 2 bp at each end. This suggests that (1) the length of the DNA does not determine the number or location of binding sites, (2) MetJ binds specifically to the portions of metboxes present and not to the junctions between metboxes, (3) MetJ binds to these partial sequences even if there is only 6 bp available, and (4) n is well determined during the fitting procedure.

Double-Metbox Binding. The double-metbox DNA oligonucleotides were titrated in a similar manner to the experiments with single-metbox DNA, and the calorimetric data were fit using the same MIS binding equations. The fit parameters for these titrations are also reported in Table 1 and indicate that both ΔG and ΔH are more negative on a per site basis than those for the single-metbox molecules and that there are two sites per duplex DNA (n = 1.87). Since each individual binding site metbox sequence is identical to that used in the single-metbox titrations, the observed increase in binding affinity suggests that there are additional factors contributing to the binding. Fitting the data to a MIS model with two types of sites results in different ΔG values for each site, suggesting cooperativity. Due to the inability of the independent site model to correctly describe positively cooperative systems (Bains & Freire, 1991), the data from these two metbox experiments were therefore interpreted in terms of other more appropriate cooperative models.

Data from the two-metbox titrations were fit reasonably with the cooperative binding model and eq 7 described

Table 1[a]

		substrate	ligand	temp (°C)	n^b	ΔG_{298} (kcal·mol^{-1})	ΔH (kcal·mol^{-1})	ΔS (cal·mol^{-1}·K^{-1})
12 bp DNA	▲	1 metbox[c]	MetJ−SAM	10.65	0.9	−8.1	−0.9	25
	■	1 metbox[c]	MetJ−SAM	25.58	0.9	−7.6	−4.1	12
	◆	1 metbox[c]	MetJ−SAM	25.12	0.8	−7.9	−4.1	13
	●	1 metbox[c]	MetJ−SAM	35.77	0.9	−7.4	−9.5	−7
	○	1 metbox[c]	MetJ	25.49	1.0	−5.3	1.3	22
	△	1 metbox[c]	MetJ	24.91	1.0	−5.5	3.3	29
	□	1 metbox[c]	MetJ−Tricine	25.04	1.0	−5.4	2.5	27
	×	random[c]	MetJ−SAM	25.82	1.6	−5.7	−2.6	10
20 bp DNA		2 metboxes[c,d]	MetJ−SAM	25.53	1.9	−8.5	−5.7	9
	■	2 metboxes[e]	MetJ−SAM	25.53	1.8	−7.6	−4.5	11
				cooperative[f]		*−0.8*	*−2.9*	*−7*
	●	2 metboxes[e]	MetJ−SAM	35.81	1.7	−7.8	−9.1	−4
				cooperative[f]		*−1.2*	*−6.8*	*−18*
	△	2 metboxes[e]	MetJ	25.32	0.9	−7.8	2.6	35
				cooperative[f]		*−0.8*	*−0.6*	*1*
		MetJ/DNA[c,g]	SAM	24.76	3.95	−6.9	−8.3	−4

[a] Individual fit parameters and graph symbols for Figures 3 and 4. [b] Binding stoichiometry, ligand molecules per substrate molecule. [c] Fit to the MIS model with one type of binding site (see Experimental Procedures). [d] MIS fit of the 25 °C double metbox plus SAM titration with MetJ, for comparison with the cooperative model fit for the same data set (below) and the single-metbox fits. [e] Fit to the cooperative model (see Experimental Procedures). [f] Intrinsic binding parameters are listed in roman type for all entries, while cooperative parameters are listed in italics. [g] Titration of the $(MetJ)_2$−DNA complex with SAM.

earlier, by an iterative procedure starting with estimated values for the thermodynamic parameters. Starting values for the noncooperative intrinsic ΔG and ΔH were taken directly from the results of the single-metbox titrations, while starting values for the cooperative terms Δg_c and Δh_c were predicted by taking the difference between the single-metbox values and the values from the MIS fit of the double-metbox data determined on a per binding site basis as shown in eqs 8 and 9. The factor of 2 standardizes the values to kilocalo-

$$\Delta g_c' = 2(\Delta G_{2\ \mathrm{metbox}} - \Delta G_{1\ \mathrm{metbox}}) \quad (8)$$

$$\Delta h_c' = 2(\Delta H_{2\ \mathrm{metbox}} - \Delta H_{1\ \mathrm{metbox}}) \quad (9)$$

ries per cooperative interaction, each of which involves two single-site binding events. Fitting was not globally convergent unless starting values near these were used, although all thermodynamic quantities could be fit as adjustable parameters from these starting points. The best-fit curves are illustrated in Figure 4. It is interesting to note that values for Δg_c, Δh_c, and ΔH derived in this way match those determined from the initial portion of the curves, in which the y intercept, determined by linear regression, represents ΔH and the most negative observed heat represents $(2\Delta H + \Delta h_c)/2$ (Bains & Freire, 1991). The results, reported in Table 1 from the best-fit curves, show that the values of ΔG and ΔH are within 6% of those measured in the single-metbox titrations, demonstrating that the affinity of MetJ for the individual metboxes is independent of DNA length. This supports the model used here in which the MetJ affinity is the same for both the 12 and the 20 base-pair oligonucleotides containing one or two metboxes, respectively. In addition, non-zero negative values were obtained for the cooperative parameters Δg_c and Δh_c in the presence of SAM. The negative value for ΔG and the positive value for ΔH in the absence of SAM also parallel the single-metbox parameters in the absence of SAM, although the cooperative Δh_c remains negative without SAM, as might be expected for the dimer-to-dimer interaction reported crystallographically (Somers & Phillips, 1992). The temperature dependence of ΔH and ΔC_p was similar to that for the single-metbox DNA. Δh_c, however, showed a stronger temperature dependence

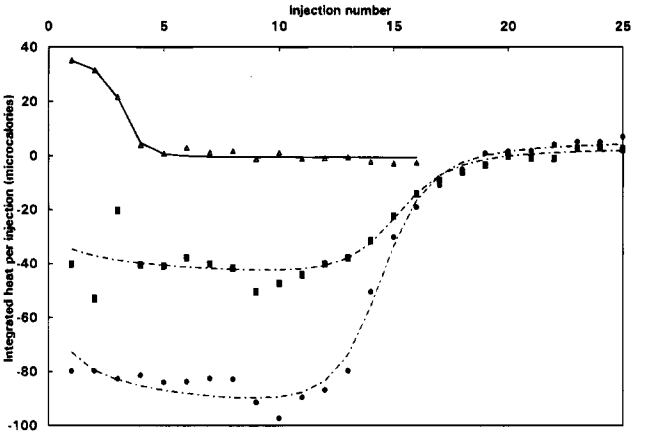

FIGURE 4: Calorimetric data and two-site cooperative fits for the double-metbox titrations with SAM at 25 °C (filled squares) and 35 °C (filled circles) and without SAM at 25 °C (open triangles). As with the 12 base-pair DNA, reactions in the presence of SAM (filled symbols) are exothermic. Although the reaction in the absence of SAM (open triangles) is endothermic and the intrinsic ΔH is positive, the cooperative enthalpy is negative even without SAM.

than ΔH, with a differential cooperative heat capacity, Δc_{pc}, in excess of 0.5 kcal·mol^{-1}·K^{-1}. The data for the experiment in the absence of cofactor were not as well fit as when SAM was present, due to the opposite signs of the intrinsic and cooperative enthalpies causing partial cancellation which reduced the intensity of the experimentally measured heats.

SAM Binding Parameters. The direct determination of the thermodynamic values for SAM binding to a MetJ−DNA complex with a single metbox is not feasible due to the inability to saturate apoMetJ with DNA based on the low binding affinity of apoMetJ and the limited solubility of the DNA. However, SAM binding to the double-metbox DNA−MetJ complex can be studied successfully since the additional cooperative binding affinity of two MetJ dimers on the adjacent DNA sites allows greater than 90% saturation to be achieved even in the absence of SAM. As studied in this case, the $(MetJ)_2$−DNA sample was at the limit of solubility. It should be pointed out that this measurement is sufficient to determine the other SAM binding values since one set of thermodynamic state functions allows the deriva-

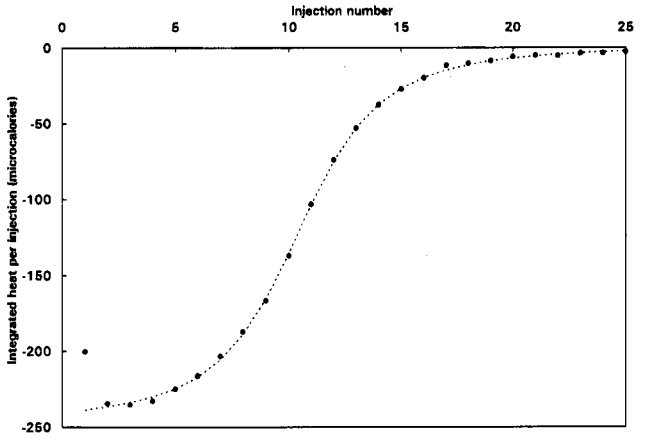

FIGURE 5: Data and MIS fit for SAM binding to MetJ complexed with double-metbox DNA.

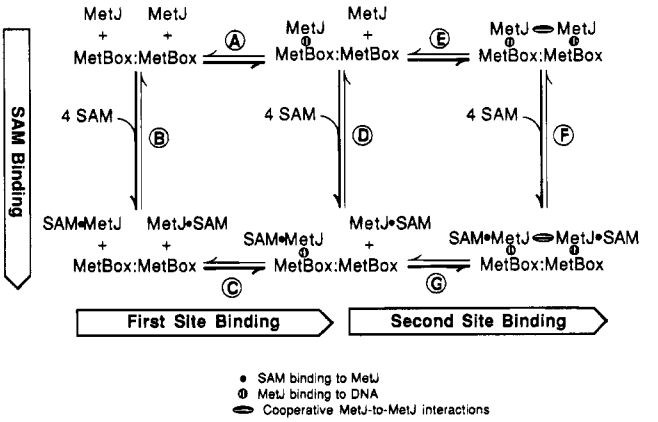

FIGURE 6: Global model thermodynamic cycle for MetJ binding, keyed to the thermodynamic parameters in Table 2. Heavier arrows indicate the direction of spontaneous reaction. Binding of MetJ to the first of two metbox sites is represented in the left half of the figure and cooperative binding of the second MetJ on the right, while SAM binding to MetJ is represented by the three vertical transitions. MetJ−SAM, MetJ−DNA, and cooperative MetJ−MetJ interactions are depicted by solid and vertically and horizontally striped circles, respectively. All transitions were measured experimentally except reactions B and D, which were derived from the other parameters. Note that reaction D consists of half-B and half-F reactions.

tion of the other thermodynamic parameters by completion of the thermodynamic cycle illustrated with the global model and Figure 6. Here the saturated $(MetJ)_2$−DNA complex was titrated with a 15 mM solution of SAM. The integrated data from the thermogram and MIS fit to the data are depicted in Figure 5. The parameters derived from the data are also reported in Table 1. Four binding sites per DNA were found as expected for one two-site DNA with two MetJ dimers bound and two SAMs bound per protein dimer. Fitting the data with higher order MIS models produced thermodynamic values for each site that were identical to the model with only one type of binding site, indicating that the binding of SAM is entirely independent and noncooperative, as reported previously (Saint-Girons et al., 1986) and that the model with only a single-site type can be used. It is interesting to note that this reaction and the cooperative protein interactions are the only equilibria in this system that have negative values of ΔS at 25 °C. Parameters for SAM binding to MetJ in the absence of DNA were then derived by completion of the thermodynamic cycle.

Global Binding Model. A global model incorporating all experimentally measured binding parameters was developed in order to describe the overall binding mechanism. In this model the overall binding process was divided into individual steps characterized by the following three separate interaction types: (1) binding of one MetJ dimer to one DNA metbox, (2) binding of SAM to MetJ, increasing the affinity for DNA binding, and (3) binding of one protein dimer to its neighboring protein dimer, the source of multiple-site cooperativity. The two-part paired thermodynamic cycle described by this system is schematically illustrated in Figure 6.

This model does not explicitly include three additional factors which are considered insignificant under the conditions of these studies: (1) repressor affinity for nonoperator DNA, since only metbox DNA was present; (2) possible SAM−DNA interactions, measured to be negligible at 2 mM SAM, but observable at concentrations of SAM greater than 10 mM; and (3) structural rearrangements due to SAM binding that might cause the ΔC_p and cooperative parameters for apoMetJ to differ from the parameters for holoMetJ, because no significant differences are seen between the three crystal structures (Rafferty et al., 1989; Somers & Phillips, 1992). Thus the model assumes that the protein structure remains relatively unchanged upon binding SAM and that the neighboring dimers contact each other through their first α helices (A helices) without altering the protein structure.

All steps in the global model were characterized by a temperature-corrected ΔG_{298} and ΔH_{298} for each of the following: (1) intrinsic single-metbox binding without SAM, (2) intrinsic single-metbox binding with SAM, (3) cooperative protein−protein interactions (the same with and without SAM), (4) SAM binding to MetJ without DNA (values determined by completion of the thermodynamic cycle), and (5) SAM binding to MetJ bound to DNA, plus (6) an intrinsic single-metbox ΔC_p (the same with and without SAM) and (7) a cooperative Δc_{pc} (the same with and without SAM). The reported similarities of crystal structures with and without SAM support the use of SAM-independent ΔC_p and cooperative parameters.

The data were fit to the global model by minimizing the sum of all the individual error figures during adjustment of the ten parameters ($4\ \Delta G + 4\ \Delta H + 2\ \Delta C_p$). The fitting was well-behaved as long as starting values near those determined from individual fits to each data set were used (Table 1). It is important to note that all values of n determined by the global fit differed less than 10% from the individually fit values and remained near 1 per metbox for the experiments in the presence of SAM. The experiments in the absence of SAM, fit to $n = 0.9 \pm 0.2$, implying that while each experimental data set is insufficient to determine n individually as experienced in the MIS and cooperative models, the four data sets combined were complete enough to determine n. The global error figure (χ^2) was reduced 40% relative to the error figure derived from averaged individual parameters. Statistically, there is an advantage in global fitting due to an increase in the number of degrees of freedom. In this case 241 points from 12 experiments were used to determine 10 thermodynamic parameters during the fitting process. The globally fit parameters reported in Table 2 therefore represent a best fit to all titration data collected in this study.

Table 2[a]

label	binding event	ΔG_{298} (kcal·mol^{-1})	ΔH_{298} (kcal·mol^{-1})	ΔS_{298} (cal·mol^{-1}·K^{-1})	ΔC_p (cal·mol^{-1}·K^{-1})
A	MetJ to first site, no SAM	-5.8 ± 0.5	2.6 ± 0.8	28 ± 4	ND[b]
B[c]	SAM to MetJ, no DNA	-6.0 ± 0.5	-4.6 ± 0.7	5 ± 4	ND
C	MetJ to first site, with SAM	-7.7 ± 0.3	-4.6 ± 0.4	10 ± 2	-290 ± 60
D[d]	SAM to $(MetJ)_1$−DNA	-6.5 ± 0.3	-6.4 ± 0.4	0 ± 2	ND
E[e]	MetJ to second site, no SAM	-7 ± 1	1 ± 2	27 ± 10	ND
F	SAM to $(MetJ)_2$−DNA	-6.95 ± 0.05	-8.23 ± 0.08	-4.3 ± 0.4	ND
G[e]	MetJ to second site, with SAM	-9 ± 1	-6 ± 2	10 ± 10	-1100 ± 300
	MetJ to MetJ interaction[f]	-1.3 ± 0.8	-2 ± 1	-2 ± 7	-800 ± 200
	MetJ to random DNA, with SAM[g]	-5.7 ± 0.2	-2.6 ± 0.4	10 ± 2	ND

[a] Globally fit values for the model in Figure 6, representing the best fit to all reported ITC data. Energies are molar quantities per ligand site, at 25 °C (per MetJ dimer in A, C, E, and G; per SAM in B, D, and F). [b] Not determined. [c] Per SAM site (there are four SAM sites throughout this representation). [d] Note that this is an average value per site representing an equal combination of the binding energies in B and F. [e] Binding energy to the second site is comprised of the first-site binding energy plus the overall cooperative energy. [f] Cooperative contribution to binding of the second MetJ molecule, independent of SAM, per mole of MetJ-to-MetJ interaction. [g] $n = 1.6 \pm 0.3$.

DISCUSSION

The titration calorimetric measurements carried out in this study yield thermodynamic values for the binding events associated with the interaction of the methionine repressor protein MetJ, the corepressor *S*-adenosylmethionine, and consensus sequence DNA. These data confirm that the affinity of MetJ for single-metbox operator DNA is weak in the absence of SAM by quantitatively evaluating the free energy for this interaction as $\Delta G = -5.8$ kcal·mol^{-1}. As determined here the interaction becomes stronger in the presence of SAM by an additional -1.9 kcal·mol^{-1} of free energy for a net ΔG of -7.7 kcal·mol^{-1}. This increase in binding energy represents an approximately 24-fold increase in K_a, similar to the previously reported 10-fold increase based of filter binding assays (Saint-Girons et al., 1988). The binding enthalpies are relatively small compared to some systems (Wiseman et al., 1989; Murphy et al., 1993), but the overall ΔG's are augmented by favorable entropic contributions of 10 cal·mol^{-1}·K^{-1} in the presence of SAM and 30 cal·mol^{-1}·K^{-1} in its absence, likely due to the favorable entropy of desolvating apolar regions of the binding sites in the bound complex. In addition, the binding enthalpies for MetJ−operator interactions show a strong dependence on temperature, with a negative ΔC_p of -0.29 kcal·mol^{-1}·K^{-1}, similar to those seen in other systems (Spolar & Record, 1994). The negative sign of ΔC_p also suggests that a decrease in macromolecular hydration helps drive the system (Wiseman et al., 1989; Murphy et al., 1993). This agrees with hydration modeling simulations, in which the macromolecules show a loss of associated water and solvent-accessible surface area upon binding. The independence of ΔH on the presence of buffer molecules with different ionization enthalpies suggests that there are no net changes in ionization of the molecules upon binding, and thus ionization does not contribute to the binding process.

The binding of SAM to the four sites in the $(MetJ)_2$−DNA complex (one two-site DNA with two dimers and two SAMs per dimer) characterized in this study is entirely independent and noncooperative, similar to findings reported previously (Saint-Girons et al., 1986). The affinity of SAM for MetJ measured here is low in the absence of DNA, $\Delta G = -6.0 \pm 0.5$ kcal·mol^{-1} versus -5.1 kcal·mol^{-1} calculated from the reported 200 μM K_d (Saint-Girons et al., 1986, 1988). The free energy of SAM binding is decreased by -1.0 kcal·mol^{-1} for a net ΔG of -7.0 kcal·mol^{-1} when the protein is bound to its cognate site, representing a 5-fold increase in the K_a for this interaction that is less than the previously suggested 10-fold increase (Saint-Girons et al., 1986; Rafferty et al., 1989; Johnson et al., 1992). The derived ΔG for SAM binding to MetJ reported here is somewhat higher, however, than the earlier reported value.

The SAM binding enthalpy of -8.23 kcal·mol^{-1} is similar to -7 kcal·mol^{-1} estimated on the basis of changes in solvent-accessible surface area that occur upon binding (Murphy et al., 1993). This suggests that favorable changes in solvation are the major source of binding enthalpy. It can also be seen from the thermodynamic parameters that the -1.9 kcal·mol^{-1} increase in MetJ−DNA binding energy caused by SAM is not small relative to the -6.0 kcal·mol^{-1} of SAM binding energy associated with its interaction, which occurs on the opposite side of the protein. This also represents a significant fraction of the -7.7 kcal·mol^{-1} binding energy in the holorepressor−DNA complex. The molecular mechanism by which SAM enhances DNA binding remains unclear, considering the crystal structure shows no rearrangements of the protein that might enhance DNA affinity upon SAM binding. One suggested mechanism is based on a general charged sphere model centered on the positively charged sulfur atoms of the SAM molecules (Old et al., 1991), but this would likely cause negative cooperativity in SAM binding to MetJ since the positive charges are only 14 Å from each other compared with the 21 Å distance to the nearest DNA oxygen. Neither positive nor negative interactions between SAM molecules are seen in this study, suggesting that the positive charge on each SAM sulfur is effectively shielded by the intervening solvent. The combination of a small protein dielectric plus a large solvent dielectric may be responsible for the SAM-dependent enhancement of DNA binding on the far face of the protein and the observed lack of negative cooperativity between nearby SAM molecules.

We have modeled the binding of a second MetJ molecule to the two-metbox DNA to be the same as the binding of the first MetJ plus cooperative effects of protein−protein interactions and assume that the cooperativity is similar for apo- and holoMetJ. These assumptions are supported by the similarity of the MetJ molecules in the crystal structures of the holorepressor and holorepressor−DNA complex and by the rotational symmetry seen between the two DNA-bound dimers in the complex (Rafferty et al., 1989; Somers & Phillips, 1992), which indicates that there are no major structural rearrangements upon binding to DNA and no

difference between the two bound dimers. The calorimetric data are also seen to be consistent with this assumption, being well fit by a model for two identical sites with positive cooperativity, with each site being similar to that in the single-metbox model. The cooperative interactions show an enhancement of DNA binding similar to the enhancement caused by SAM binding, approximately -1.3 kcal·mol^{-1} of dimer−dimer interaction. The comparatively small ΔG of cooperativity derives almost totally from the associated ΔH with only a small calculated negative entropic contribution from cooperativity (-1 ± 7 cal·mol^{-1}·K^{-1}), despite the burial of hydrophobic surface area. This is most likely due to a compensating loss of motional freedom at the dimer−dimer interface. In addition, there is a significant ΔC_p for cooperativity of -0.8 kcal·mol^{-1}·K^{-1}, larger than that seen for the protein−DNA interactions and again consistent with decreases in hydration helping to drive the cooperative effects, also seen in our hydration modeling study.

The positive ΔH of binding in the absence of SAM is an unusual feature of this system. DNA binding is enthalpically unfavorable until SAM binds, but cooperativity is always enthalpically favored. The enthalpic barrier to apoMetJ binding to DNA is compensated by a large entropic contribution, likely due to high mobility in the weakly bound complex in combination with unfavorable solvation of the binding interface when not bound (Murphy et al., 1993; Wiseman et al., 1989). The ΔC_p's of binding and cooperativity most likely derive from solvation effects. These are all nonspecific effects, but it should be noted that the crystal structure of the complex shows that water is bound in the protein−DNA interface (Somers & Phillips, 1992), implicating a specific role for water in recognition in addition to nonspecific contributions to binding.

The results presented here are not directly comparable quantitatively with those communicated recently due to differences in experimental conditions and binding models (Cooper et al., 1994). One factor that bears on interpretation of the thermodynamic parameters in that report associated with the binding of SAM to the $(MetJ)_2$−DNA complex is the conclusion from our work that the MetJ in the complex studied by Cooper et al. was not saturated with DNA. Therefore, a number of concerted binding reactions might be expected in the experiment, which were not accounted for in the analytical model. The results presented here reinforce this suggestion since the additional binding contributions from MetJ interacting with DNA would be detected as an increase in the apparent exothermicity of the reaction similar to that measured. Nevertheless, the ΔG reported here of -6.95 ± 0.05 kcal·mol^{-1} for the binding of SAM to the $(MetJ)_2$−DNA complex is only approximately 0.2 kcal·mol^{-1} lower than the Cooper value of -6.8 kcal·mol^{-1}. On the basis of this analysis, we favor our values for ΔH of SAM binding which is -8.23 ± 0.08 kcal·mol^{-1} or some 2.8 kcal·mol^{-1} less exothermic than that reported by Cooper et al.

Likewise, we also conclude that the recently reported titrations of MetJ into DNA were likely not saturated with SAM at the concentration of 0.288 mM SAM reported (Cooper et al., 1994). Under these conditions multiple binding events, not included in the binding model used, are expected which will result in an apparent binding enthalpy that is higher than that measured under saturating conditions. This may account for the differences we observe for the total ΔG and ΔH of -9 ± 1 and -6 ± 2 kcal·mol^{-1}, respectively, determined for a cooperative model compared with values of -10 and -24 kcal·mol^{-1} reported for a noncooperative model by Cooper et al. The earlier data, however, show the same small cooperative curvature in the pretransition portion of the titrations observed here, suggesting that a cooperative model like that used here would be appropriate.

The results from this study help illuminate the repression mechanism of MetJ by suggesting how a stable repression complex might form *in vivo*. There is a small but measurable affinity of the protein for random DNA, which suggests that in the cell nonspecific binding of MetJ to any DNA occurs, increasing the local concentration of MetJ around the DNA of the cell. This initial nonspecific binding is weak and therefore relatively unstable. The nonspecific interactions, however, enhance the probability of the MetJ encountering an operator sequence.

Similarly, since the affinity of MetJ for SAM is relatively low, its population is largely in the apoMetJ form within the cell. If either the DNA-bound apoMetJ or the non-DNA-bound holoMetJ encounters its other cognate molecule, a complex of intermediate stability is formed. This single-dimer holorepressor complex can then go on to be further stabilized by cooperative interactions should another MetJ (apo or holo) bind to a neighboring metbox, forming a stable and long-lived complex competent for repression. *In vivo*, the combination of SAM binding and cooperative protein−protein interactions creates a high-affinity bound complex, which continues to increase in strength as additional MetJ dimers bind to additional contiguous metboxes.

The low affinity of SAM for MetJ implies that repression is only sensitive to very high levels of SAM, under which methylation pathways might be driven to overmethylation and cause damage to the cell. The large increase in DNA binding affinity upon formation of holorepressor suggests that even small amounts of MetJ protein are sufficient for repression when large amounts of SAM are present to saturate MetJ. These qualities allow a continuously variable, progressive response to cellular conditions, with binding remaining in the lower, logarithmically responsive end of the binding curve. This mechanism is distinct from a simple on/off switch. Multiple-metbox and nonconsensus operator sites may have evolved in preference to operators with fewer sites to fine-tune the feedback sensitivity and dynamic range of the repression system.

ACKNOWLEDGMENT

The authors thank Dr. Kip Murphy, Dr. Dong Xie, and Ms. Marina Kasimova for their help in design, performance, and analysis of the ITC experiments and especially for their dedication to teaching the fine art of titration calorimetry. We also thank Dr. Mike Johnson for use of his program Nonlin and Dr. David Myers for his help in its programming. We gratefully acknowledge Dr. Tom Kirby and Dr. Ron Greene for providing us their overproducing MetJ plasmid pET-MetJ and for access to their data prior to publication. This work was carried out (in part) at the Biocalorimetry Center, a Biomedical Research Technology Resource Center sponsored by the National Institutes of Health (RR04328), Department of Biology, Johns Hopkins University, Baltimore, MD.

SUPPLEMENTARY MATERIAL AVAILABLE

A more detailed description of the multiple independent site binding model used in this study (8 pages). Ordering information is given on any current masthead page.

REFERENCES

Bains, G., & Freire, E. (1991) *Anal. Biochem. 192*, 203−206.

Belfaiza, J., Parsot, C., Martel, A., Bouthier de la Tour, C., Margarita, D., Cohen, G. N., & Saint-Girons, I. (1986) *Proc. Natl. Acad. Sci. U.S.A. 83*, 867−871.

Brandts, J. F., & Lin, L.-N. (1990) *Biochemistry 29*, 6927−6940.

Cantor, C., & Schimmel, P. R. (1980) *The Behavior of Biological Macromolecules*, W. H. Freeman and Co., San Francisco.

Cohen, G. N., & Jacob, F. (1959) *C. R. Acad. Sci. Paris 248*, 3490−3492.

Cooper, A., McAlpine, A., & Stockley, P. G. (1994) *FEBS Lett. 348*, 41−45.

Davidson, B. E., & Saint-Girons, I. (1989) *Mol. Microbiol. 3*, 1639−1648.

Edelhoch, H. (1967) *Biochemistry 6*, 1948−1954.

Freire, E., Mayorga, O. L., & Straume, M. (1990) *Anal. Chem. 62*, 950A−959A.

He, Y.-Y., McNally, T., Manfield, I., Navratil, O., Old, I. G., Phillips, S. E. V., Saint-Girons, I., & Stockley, P. G. (1992) *Nature 359*, 431−433.

Johnson, C. M., Cooper, A., & Stockley, P. G. (1992) *Biochemistry 31*, 9717−9724.

Johnson, M. L. (1983) *Biophys. J. 44*, 101−106.

Johnson, M. L., & Frasier, S. G. (1985) *Methods Enzymol. 117*, 301−342.

Kirby, T. W., Hindenach, B. R., & Greene, R. C. (1986) *J. Bacteriol. 165*, 671−677.

Murphy, K. P., Xie, D., Garcia, K. C., Amzel, L. M., & Freire, E. (1993) *Proteins: Struct., Funct., Genet. 15*, 113−120.

Old, I. G., Phillips, S. E. V., Stockley, P. G., & Saint-Girons, I. (1991) *Prog. Biophys. Mol. Biol. 56*, 145−184.

Phillips, S. E. V. (1991) *Curr. Opin. Struct. Biol. 1*, 89−98.

Phillips, S. E. V., Manfield, I., Parsons, I., Davidson, B. E., Rafferty, J. B., Somers, W. S., Margarita, D., Cohen, G. N., Saint-Girons, I., & Stockley, P. G. (1989) *Nature 341*, 711−715.

Phillips, S. E. V., Boys, C. W. G., He, Y.-Y., Manfield, I., McNally, T., Navratil, O., Old, I. G.; Phillips, K., Rafferty, J. B., Somers, W. S., Strathdee, S., Saint-Girons, I., & Stockley, P. G. (1993) *Nucleic Acids Mol. Biol. 7*, 28−46.

Press, W. H., Teukolsky, S. A., Vetterling, W. T., & Flannery, B. P. (1992) *Numerical Recipes in Fortran: The Art of Scientific Computing*, Cambridge University Press, Cambridge.

Rafferty, J. B., Somers, W. S., Saint-Girons, I., & Phillips, S. E. V. (1989) *Nature 341*, 705−710.

Saint-Girons, I., Duchange, N., Cohen, G. N., & Zakin, M. M. (1984) *J. Biol. Chem. 259*, 14282−14285.

Saint-Girons, I., Belfaiza, J., Guillou, Y., Perrin, D., Guiso, N., Bârzu, O., & Cohen, G. N. (1986) *J. Biol. Chem. 261*, 10936−10940.

Saint-Girons, I., Parsot, C., Zakin, M. M., Bârzu, O., & Cohen, G. N. (1988) *CRC Crit. Rev. Biochem. 23* (Suppl. 1), S1−S42.

Smith, A. A., Greene, R. C., Kirby, T. W., & Hindenach, B. R. (1985) *Proc. Natl. Acad. Sci. U.S.A. 82*, 6104−6108.

Somers, W. S., & Phillips, S. E. V. (1992) *Nature 359*, 387−393.

Spolar, R. S., & Record, M. T., Jr. (1994) *Science 263*, 777−784.

Stramue, M., & Freire, E. (1992) *Anal. Biochem. 203*, 259−268.

Studier, F. W., & Moffatt, B. A. (1986) *J. Mol. Biol. 189*, 113−130.

Weissbach, H., Greene, R. C., Saint-Girons, I., Cohen, G. N., et al. (1985) *BioEssays 3*, 210−213.

Wiseman, T., Williston, S., Brandts, J. F., & Lin, L. (1989) *Anal. Biochem. 179*, 131−137.

Wyman, J., & Gill, S. J. (1990) *Binding and Linkage: Functional Chemistry of Biological Macromolecules*, University Science Books, Mill Valley, CA.

BI942009H